Article

Glutathione Reductase-Sensitive Polymeric Micelles for Controlled Drug Delivery on Arthritic Diseases

Ana Cláudia Lima, Rui L. Reis, Helena Ferreira, and Nuno M. Neves*

Cite This: https://doi.org/10.1021/acsbiomaterials.1c00412

Read Online

ACCESS | 📊 Metrics & More | 📰 Article Recommendations

ABSTRACT: Inflammation plays an essential role in arthritis development and progression. Despite the advances in the pharmaceutical field, current treatments still present low efficacy and severe side effects. Considering the high activity of the glutathione reductase (GR) enzyme in inflamed joints, a distinctive drug delivery system sensitive to the GR enzyme was designed for efficient drug delivery on arthritic diseases. A linear amphiphilic polymer composed of methoxypolyethylene glycol amine-gluta-thione-palmitic acid ($mPEG-GSH_n-PA$) was synthesized and the intermolecular oxidation of the thiol groups from GSHs retain the drug inside the resulting micelles. Stable polymeric micelles of 100 nm of size presented a loading capacity of dexamethasone (Dex) up to 65%. Although in physiological conditions the Dex release presented slow and sustained kinetics, in the presence of the GR enzyme, there was a burst release (stimuli-responsive properties). Biological assays demonstrated their cytocompatibility in contact with human articular chondrocytes, macrophages, and endothelial cells as well as their hemocompatibility. Importantly, in an in vitro model of inflammation, the polymeric micelles promoted a controlled drug release in the presence of GR, exhibiting a higher efficacy than the free Dex while reducing the negative effects of the drug into normal cells. In conclusion, this formulation is a promising approach to treat arthritic diseases and other inflammatory conditions.

KEYWORDS: *polymeric micelles, enzymatic-sensitive micelles, inflammation targeting, controlled release, arthritic diseases*
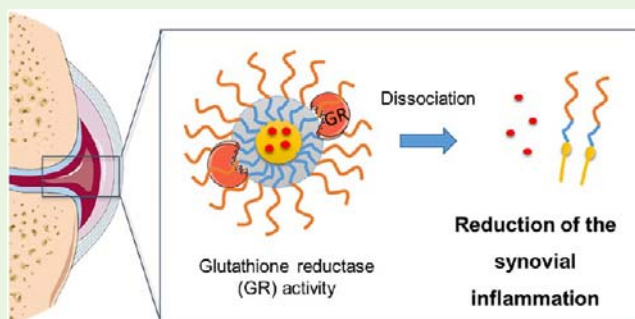
Arthritic diseases comprise more than 150 different joint disorders characterized by joint and/or musculoskeletal system inflammation.[1] Their most common forms are osteoarthritis (OA) and rheumatoid arthritis (RA), which are associated with chronic synovial inflammation, pain, and tissue damage.[2] Arthritis affects more than 350 million people worldwide, and because of the increase in the proportion of the elder population, their incidence and prevalence are also increasing. Moreover, these diseases are one of the leading causes of work disability and loss of quality of life because of their painful, chronic, and incapacitating features.[3]

Because arthritis has no cure,[4] current treatments include nonsteroidal anti-inflammatory drugs (NSAIDs) and gluco-corticoids (GCs), for instance, dexamethasone (Dex) and prednisolone, for OA and RA and disease-modifying antirheumatic drugs (DMARDs) and biologicals therapies for RA (still in clinical trials for OA).[5] Particularly, GCs present potent anti-inflammatory and immune-suppressive actions, being among the most commonly prescribed drugs for various inflammatory, autoimmune, and allergic disorders.[6] Nevertheless, the ubiquitous expression of the GC receptors limit their therapeutic efficiency, with an off-targeted biodistribution profile and low local drug bioavailability.[7,8] Additionally, their

serious side effects, such as osteoporosis and hyperglycemia, severely hamper GCs' clinical application.

Recently, several efforts have been made to develop nanomedicines that improve the accumulation of the drug in the target inflamed tissue.[8−11] As polymeric micelles present good biocompatibility, high stability, and the ability to increase the drug bioavailability and accumulation in target tissues, they have been widely used as drug delivery systems (DDS).[12−14] Indeed, they can effectively encapsulate a wide variety of biological agents, controlling their distribution and function in the body.[7,15]

One of the most promising concepts in the drug delivery field involves the design of nanomedicines with tunable properties that can be engineered to respond to the pathophysiological parameters of the diseased tissues, and consequently, by controlling the spatiotemporal distribution of

A

Scheme 1. Schematic Illustration of the Glutathione Reductase-Sensitive Polymeric Micelles Rationale for Arthritis Treatment[a]
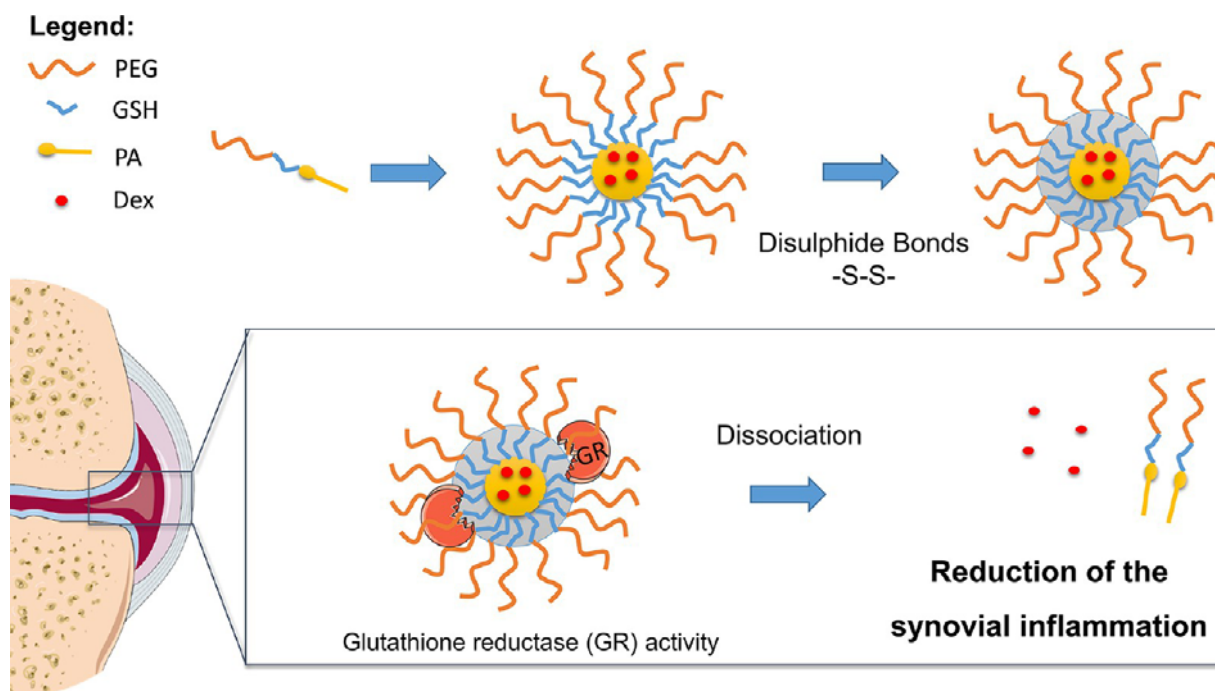
[a]Abbreviations: PEG, polyethylene glycol; GSH, glutathione; PA, palmitic acid; Dex, dexamethasone.

the drugs, extend their therapeutic index.[16,17] In this study, glutathione reductase (GR)-sensitive polymeric micelles were explored to promote a controlled drug delivery on arthritic diseases. Glutathione (GSH) is the key regulator of the intracellular redox state, presenting an essential role in the detoxification of reactive oxygen species and peroxides.[18,19] In those reactions, two GSH are oxidized to form glutathione disulfide (GSSG) via disulfide bond. In its turn, GSSG can be reduced by GR enzyme to regenerate GSH. Taking into consideration the higher activity of GR in the synovial fluid of RA and OA patients, in comparison with normal controls,[20,21] this enzyme can selectively stimulate the controlled drug release in inflamed joints. Additionally, the higher permeability and angiogenesis of arthritic patients enhance a targeted (passive) drug delivery to the inflamed sites through the mechanism of extravasation via leaky vessels and subsequent inflammatory cell-mediated sequestration (ELVIS).[22−24]

Polymeric micelles were made of methoxypolyethylene glycol amine-glutathione-palmitic acid (mPEG-GSH$_n$-PA) polymers. As PEG avoids the adsorption of opsonin proteins to nanoparticles (NPs), it is extensively used in the pharmaceutical and nanotechnology fields.[7] Indeed, PEG reduces the immunogenicity of therapeutic formulations, increases their pharmacokinetic profile, and decreases the unspecific biodistribution.[25,26] Moreover, GSH and PA have been used to produce polymeric micelles.[27−32]

Hence, this study proposes a nanocarrier intended for the controlled delivery of an anti-inflammatory drug (Scheme 1). After systemic administration, polymeric micelles will be passively accumulated in the articular inflamed joint through the ELVIS effect. Once in the joints, GR activity will destabilize the micellar structure via a thiol−disulfide exchange, triggering the release of the encapsulated drug from the micelles. Considering the current limitations of GC treatments,

this is a promising strategy to enhance the drug therapeutic efficacy while reducing their systemic side effects.

■ EXPERIMENTAL SECTION

Materials. Unless otherwise noted, all chemicals were purchased from Sigma-Aldrich (USA), including Dex (D1756, purity ≥98% by HPLC). RPMI-1640 medium and fetal bovine serum (FBS) were acquired from Thermo Fisher Scientific (USA). Human IL-6 and TNF-α standard ABTS ELISA development kits and human fibroblast growth factor (bFGF) were purchased from Peprotech (USA).

Synthesis of mPEG-GSH$_n$-PA Amphiphilic Polymers. To prepare mPEG-GSH$_n$-PA polymers, in the first step, we reacted mPEG (0.01 mmol) and GSH (0.02 mmol) in ultrapure water for 24 h at room temperature (RT), using 1-(3-(dimethylamino)propyl)-3-ethylcarbodiimide/N-hydroxysuccinimide (EDC/NHS) at 50/200 mM in MES hydrate (pH 4.7) as coupling agents. To remove the unreacted compounds, we placed the product of the reaction in dialysis systems with 3.5−5 kDa cutoff for 8 h at RT (with 4 ultrapure water exchanges). Afterward, the water was removed by freeze-drying. In the second step, mPEG-GSH$_n$ reacted with PA (0.011 mmol) in tetrahydrofuran (THF) using 1H-benzotriazole-1-yl)-1,1,3,3-tetramethylaminium tetra fluoroborate (TBTU, 0.011 mmol) and triethylamine (TEA, 0.02 mmol) for 24 h at RT.

Micelle Production and Dex Encapsulation. For micelle production, 5 mL of the polymers solution in THF was added dropwise at 1 mL/min of rate to 20 mL of ultrapure water, and the THF was removed with strong magnetic stirring (600 rpm) for 48 h at RT. Unreacted compounds were eliminated by two washing steps with ultrapure water and centrifugation (45 min, 5000 rpm, 20 °C) by Vivaspin 300 kDa Filter Units (Fisher Scientific, USA). The final micellar volume was 8 mL (1 mg/mL of polymer concentration).

For drug encapsulation, Dex was dissolved in the THF solution, before micelle production as previously described.

Micelle Characterization. Several testing methods were conducted to demonstrate the main physical and chemical properties of the developed polymeric micelles.

Chemical Characterization. The chemical structures of all the products were identified by proton nuclear magnetic resonance (¹H

NMR) and Fourier-transform infrared spectroscopy (FTIR). For ^{1}H NMR analysis, polymeric micelles, PEG, and GSH were solubilized in deuterium oxide, whereas PA was solubilized in dimethyl sulfoxide-D6. A Bruker AVANCE 400 spectrometer was used to obtain NMR spectra, which were analyzed using the *MestReNova* software 9.0. For FTIR analysis, an IRPrestige 21 spectrometer (Shimadzu, Japan) was used to analyze the compounds by the KBr-disk method (400−4000 cm^{-1}). Besides, the amount of GSH in the polymer was determined using a thiol and sulfide quantitation kit (Invitrogen, Molecular Probes, USA). After regenerating GSSH into GSH using GR enzyme as previously described,[33] the kit was performed following the manufacturer's instructions. The absorbance was measured at 410 nm using a microplate reader (Synergy HT, BioTek, USA), being the standard curve used to infer the thiol (GSH) concentration of the samples.

Size Distribution and Zeta Potential Measurements. Intensity-distribution size and zeta-potential values were assessed by dynamic light scattering (DLS) and laser Doppler electrophoresis, respectively, using a Zetasizer Nano ZS instrument (Malvern Instruments, Portugal). DLS measurements were performed at an angle of 173° and at a wavelength of 633 nm in disposable polystyrene cuvettes, whereas zeta potential was accomplished using a dip cell. All the measurements were performed at 25.0 ± 0.1 °C.

For storage stability, empty polymeric micelles were kept at 4 °C under static conditions. The size, polydispersity index (PDI), and zeta potential was determined during the experimental time of 6 months, as described above.

Polymeric Micelle Morphology. The polymeric micelle morphology was assessed by scanning electron microscopy (SEM). After air-drying the polymeric micelles at the surface of a glass slide, they were sputter-coated with palladium (EM ACE600, LEICA), and then analyzed using high-resolution field-emission SEM (Auriga Compact, Zeiss, Germany).

Drug Entrapment Efficiency. The Dex loading content in the polymeric micelles was performed with micelle:Dex feed weight ratios between 1:0.2 and 1:0.8 at a micelle concentration (polymers concentration) of 1 mg/mL. The nonencapsulated Dex was measured in the supernatant diluted in ethanol (0.5:0.5 v/v) using UV spectroscopy (Shimadzu, Japan) at 240 nm, as previously reported.[34]

Entrapment efficiency (EE) and drug loading (DL) were calculated using the equations below:

$$\%EE = \frac{(\text{initial concentration} - \text{nonencapsulated drug})}{\text{initial concentration}}100$$

(1)

$$\%DL = \frac{\text{loaded drug mass}}{\text{total micelle mass}}100$$

(2)

In Vitro Drug Release Profile. The in vitro Dex release profiles of micelles under different external conditions were performed through the dialysis method. Briefly, 5 mL of micelle suspension was added to a dialysis system (Micro Float-A-Lyzer, 3.5−5 MWCO) that was added to a tube containing 15 mL of PBS (pH 7.4, 37 °C) and shaken at 100 rpm. At the defined time points, an aliquot (0.5 mL) was retrieved from the external tube with equal volume refill. After dilution of the aliquot with 0.5 mL of ethanol, the Dex concentration was measured using UV−vis spectroscopy equipment (Shimadzu, Japan), with Dex concentration then measured as previously described. The enzymatic-sensitiveness properties of the polymeric micelles were evaluated by adding 50 mU of GR, 0.14 mM nicotinamide-adenine dinucleotide phosphate (NADPH), and 0.1 mM ethylenediaminetetraacetic acid (EDTA) to the PBS.[21] More-over, the size distribution (size and PDI) of the polymeric micelles was evaluated over time.

Biological Assays. To assess the cytocompatibility of the developed micelles and their biological effects after encapsulation of Dex, it was performed cell isolation and culture, viability, proliferation, protein content, and morphology analysis as herein described.

Isolation and Cell Culture. Human articular chondrocytes (hACs) were isolated by enzymatic digestion, as previously described.[35] Knee

cartilage samples, collected from arthroplasty surgeries, were obtained in accordance with the 67/CA Protocol established between the Centro Hospitalar do Alto Ave, Guimarães, Portugal, and the 3B's Research Group, and after informed donor consent. hACs were cultured in DMEM high glucose (D5671), supplemented with 10% FBS, 10 mM of L-lanyl-L-glutamine, MEM with nonessential amino acids, and HEPES buffer, 100 units/mL of penicillin, 100 μg/mL of streptomycin, and 10 ng/mL of human bFGF.

Human umbilical vein endothelial (EA.hy926) cell line was cultured in DMEM low glucose (D5523) supplemented with 10% FBS, 100 units/mL of penicillin, and 100 μg/mL of streptomycin.

The human monocytic cell line THP-1 was maintained in complete RPMI (cRPMI) that consist of RPMI-1640 media supplemented with 2 mM L-glutamine, 100 units/mL of penicillin, 100 μg/mL of streptomycin, 10 mM HEPES buffer, and 10% FBS.

Cells were incubated in a humidified 5% CO$_2$ atmosphere at 37 °C.

Polymeric Micelle Cytocompatibility. Primary hACs and EA and THP-1 cell lines were used to evaluate the cytocompatibility of the polymeric micelles. hACs and EA were cultured at 5×10^4 cells/well. THP-1 was seeded at 5×10^5 cells/well with 100 nM phorbol 12-myristate-13-acetate (PMA) for 24 h. After three washes, THP-1 cell line was incubated for a further 48 h in cRPMI without PMA. Then, to obtain M1 activated macrophages, cells were stimulated with 100 ng/mL of lipopolysaccharide (LPS) during 24 h. For all the cell types, it was used an increasing concentration of the polymeric micelles sterilized through 0.22 μm filters. The cells cultured without the micelles (only culture medium) were used as controls. After 1, 3, and 7 days of culture, the different samples in triplicate were rinsed with sterile PBS and analyzed regarding cell viability, cell proliferation, protein synthesis, and cell morphology.

Cells metabolic activity was determined by Alamar blue (AB) reagent (Bio-Rad, USA), according to the instructions of the manufacturer. Briefly, after adding a medium containing 10% AB, cells were incubated for 4 h at 37 °C in a humidified 5% CO$_2$ atmosphere. The fluorescence was measured using an excitation wavelength of 530/25 nm and an emission wavelength of 590/35 nm, in a microplate reader (Synergy HT, BioTek, USA).

Cells proliferation was determined by DNA quantification using a fluorimetric dsDNA quantification kit (Quant-iT, PicoGreen, Invitrogen, Molecular Probes, USA). Briefly, samples were thawed, sonicated for 15 min, and added to a 96-well plate (Falcon). Besides the addition of 28.7 μL of sample or standard ($n = 3$), 71.3 μL of PicoGreen solution, and 100 μL of Tris-EDTA (TE) buffer were incubated for 10 min in the dark. Then, the fluorescence of each sample was measured using excitation/emission wavelengths of 485/528 nm, respectively, in a microplate reader (Synergy HT, BioTek, USA). Sample concentration was inferred from the standard curve.

The protein concentration was determined using a Micro BCA protein assay kit (Thermo Scientific, Pierce, USA), according to the manufacturer's instructions. Briefly, 150 μL of samples or standards were incubated for 2 h at 37 °C with 150 μL of working reagent in a 96-well plate. The absorbance was measured at 562 nm using a microplate reader (Synergy HT, BioTek, USA), with sample concentration being inferred from the standard curve.

Cell morphology was assessed by SEM. Briefly, after fixating the cells with 2.5% glutaraldehyde, samples were dehydrated using increasing concentrations of ethanol (20, 40, 60, 80, 90, and 100%). After sputter-coating (EM ACE600, LEICA) with a thin layer (8−12 nm) of palladium, samples were analyzed by high-resolution field-emission SEM. Microphotographs were recorded at 5 kV with magnifications of 200, 1000, and 10 000×.

Biological Effects of the Polymeric Micelles. A coculture system was used to assess the biological effects of the micelles encapsulating Dex. hACs and THP-1 cell line were seeded as previously described, being the THP-1 seeded in cell culture inserts (pore size: 1 μm) at 2.5 $\times 10^5$ cells/well. The inserts were transferred to the hACs culture, and the THP-1 cell line was stimulated to the activated M1 macrophages by adding 100 ng/mL of LPS. After 2 h of stimulation, three different conditions were tested: (i) no treatment, (ii) micelles encapsulating Dex, and (iii) free Dex. Those conditions were also tested in the hACs
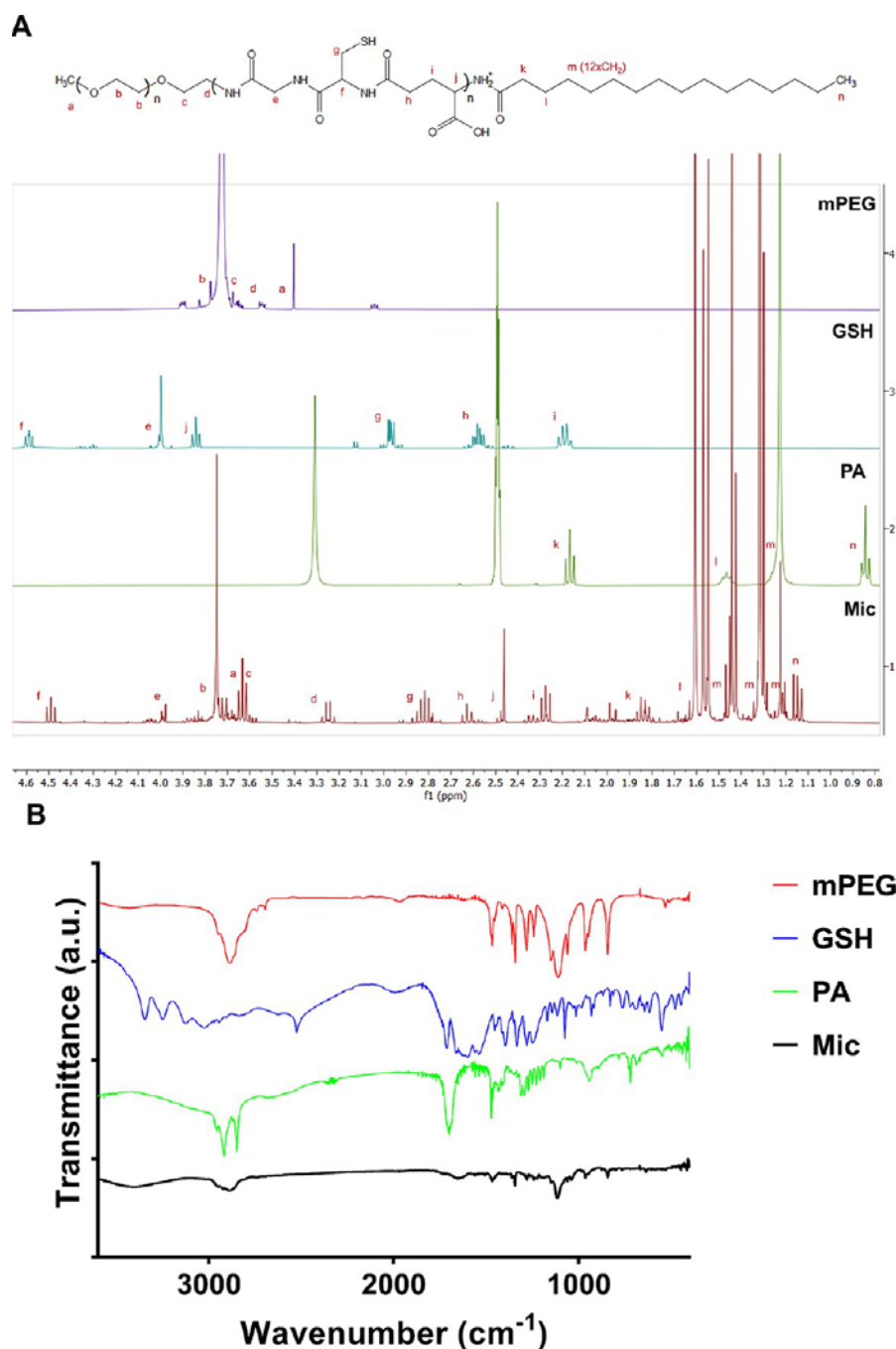
Figure 1. (A) ^{1}H NMR spectra and (B) FTIR analysis of the methoxypolyethylene glycol (mPEG), glutathione (GSH), palmitic acid (PA), and the micelles (Mic).

and activated M1 macrophages (THP-1 cells) seeded alone (monoculture). GR enzyme was added to the coculture system at 50 mU (no GR was added to the monocultures). After 1, 3, 7, and 14 days of culture, the samples were evaluated regarding cell viability, proliferation, and morphology, as described above. IL-6 and TNF-α in the media were quantified by ELISA. To keep the micelles in contact with the cells, 300 μL of fresh media was added every 3 days, but no media were removed during the time of the experiment.

Cytokine Quantification. The pro-inflammatory cytokines IL-6 and TNF-α were quantified using human sandwich ELISA kits, which were performed according to the manufacturer procedure. Cytokine concentration was inferred from the standard curve.

Hemolytic Properties. To determine the hemolytic properties of the polymeric micelles, we determined the concentration of free hemoglobin after incubating the polymeric micelles with whole human blood. Briefly, diluted blood (in saline solution (1:100) with EDTA) was incubated with increasing concentrations of the polymeric micelles, under gentle agitation for 4 h at 37 °C. Then, the hemoglobin assay kit (MAK115) was used to quantify the concentration of free hemoglobin in the samples' supernatant (samples centrifugation for 10 min at 1000 g), according to the instructions of the manufacturer. The blood in saline solution and water were used as negative and positive controls, respectively. The absorbance (A) was measured at 400 nm in a microplate reader (Synergy HT, Bio-Tek, USA). Hemoglobin concentration (C) was calculated according to the following equation:

$$C = \frac{(A_{400}\text{sample}) - (A_{400}\text{blank})}{(A_{400}\text{calibrator}) - (A_{400}\text{blank})} 100 \text{ mg/dL·df} \tag{3}$$
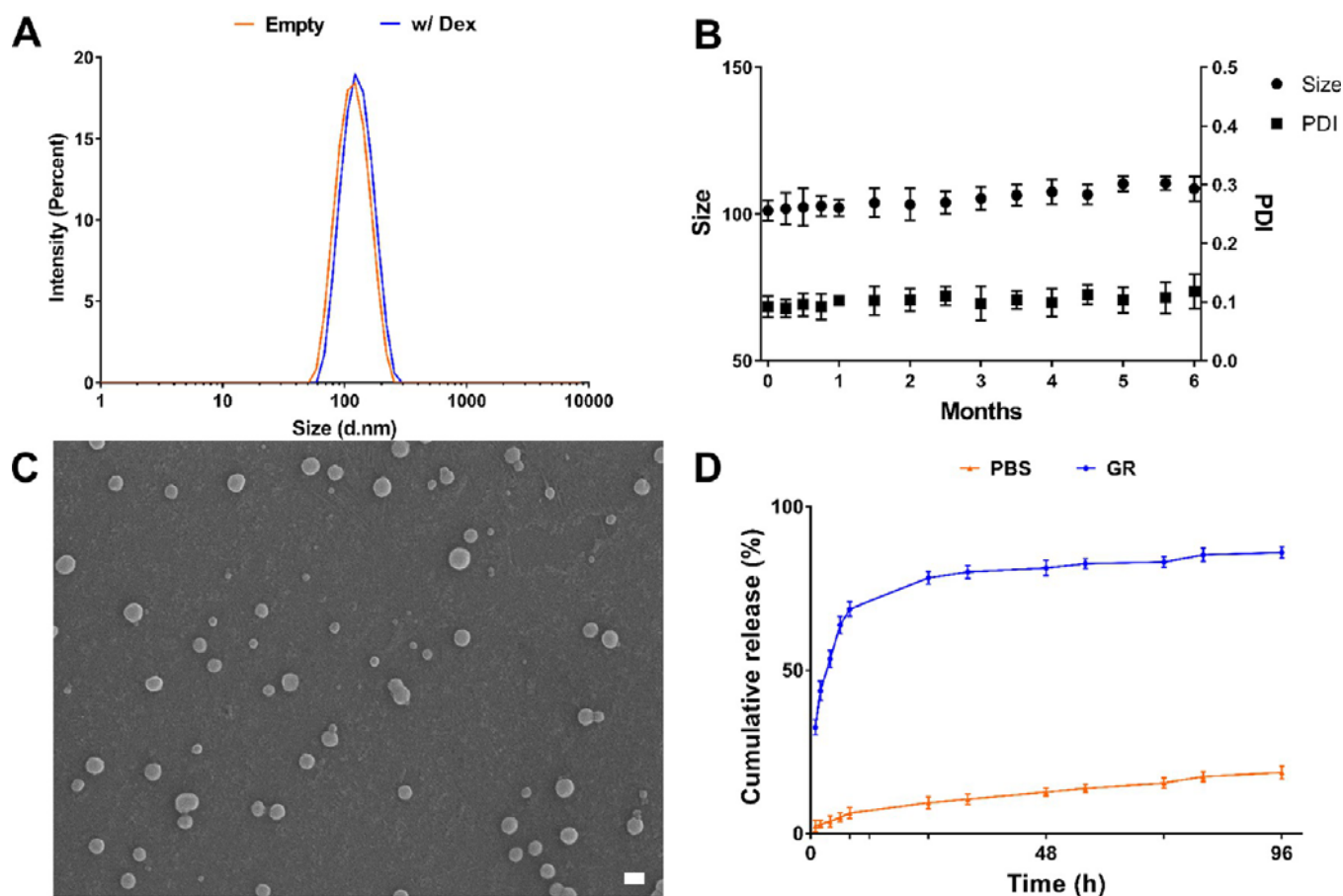
Figure 2. (A) Size distribution of the 1 mg/mL micelles without and encapsulating 4.65 mg of dexamethasone (Dex). (B) Evaluation of the size stability of the empty polymeric micelles during 6 months at 1 mg/mL. (C) SEM microphotographs of the empty polymeric micelles (scale bar: 100 nm). (D) Release profile of Dex from the 1 mg/mL micelles (encapsulating 4.65 mg of Dex) when exposed to different environments: PBS and 50 mU of glutathione reductase (GR) enzyme at 37 °C.

where, 100 mg/dL = concentration of the diluted calibrator and df = dilution factor.

Subsequently, the following equation was used to calculate the percentage of hemolysis in the samples:

$$\text{hemolysis (\%)} = \frac{C(\text{sample}) - C(\text{negative control})}{C(\text{positive control}) - C(\text{negative control})} 100$$

(4)

Statistical Analyses. The mean ± standard deviation of at least three independent assays (n = 3, average of three different measurements of, at least, three micelles populations prepared independently) are presented. Statistical analyses were performed using the GraphPad Prism Software. First, a Shapiro−Wilk test was used to access the normality of the data. As the results did not follow a normal distribution, it was performed the Kruskal−Wallis test (a nonparametric test) followed by Dunn's test. Statistically significant was considered with $p < 0.01$.

■ RESULTS

Polymeric Micelle Characterization. The synthesis of the amphiphilic polymer compromises two-step reactions: in the first, the amine groups (NH_2) of mPEG reacted with the carboxylic groups (COOH) of GSH (free NH_2 groups of GSH can also react with COOH groups of GSH, producing mPEG-GSH_n), and in the second step, the free NH_2 groups of GSH reacted with the COOH groups of PA. ^1H NMR spectra of the single compounds yielded well-defined signals (Figure 1A) similar to the ones present in databases. Importantly, in the

spectrum of the micelles, the presence of the peaks from all initial products (mPEG, GSH, PA) was observed, corroborating the synthesis of the polymer. Importantly, carbon d shifted from a multiplet in mPEG for a quartet in the micelles and the carbon j shifted from a triplet in GSH to a doublet in the micelles. In addition, the micelle spectrum presented some impurity peaks (especially around 2.1−1.9 ppm). FTIR analysis of the micelles (Figure 1B) showed a shift of the NH_2 group from the mPEG and GSH (N−H stretch absorptions at 3300−3000 cm^{-1}) to amide in the micelles (N−H stretch absorption at 3300 cm^{-1} and a C=O peak at 1680−1630 cm^{-1}). Moreover, while the GSH present a weak thiol (S−H) peak at 2550−2620 cm^{-1}, the micelles presented a weak disulfide (S−S) peak at 700−550 cm^{-1}. Besides, there is 1.86 μM of GSH in each mg of the polymeric micelles determined by the ultrasensitive thiol and sulfide colorimetric assay.

The size of the empty micelles (Figure 2A) was 101.3 ± 3.4 nm with a PDI value of 0.092 ± 0.011 and a zeta potential of −20.2 ± 3.42 mV, and these values were stable for at least 6 months (Figure 2B). From SEM microphotographs (Figure 2C), polymeric micelles presented a spherical shape with a diameter of ca. 100 nm, which is in agreement with DLS measurements.

Efficacy of Drug Encapsulation and in Vitro Release Kinetics. Dex loading content and entrapment efficiency increased directly with the micelle:Dex feed weight ratio,

reaching a maximum of 64% in the 1:0.8 condition (Table 1). After the drug was encapsulated, polymeric micelles presented 118.8 ± 0.2 nm size (Figure 2A), with 0.105 ± 0.009 of PDI and −17.4 ± 2.7 mV of zeta potential.

Table 1. Dex Loading Content (in mg and %) and Entrapment Efficiency (in %) into the Micelles at a Concentration of 1 mg/mL

micelles:Dex feed weight ratio	Dex loading content (mg)	Dex loading content (%)	entrapment efficiency (%)
1:0.2	0.57 ± 0.03	7.06 ± 0.38	35.3 ± 1.9
1:0.4	1.38 ± 0.08	17.21 ± 1.05	39.8 ± 1.3
1:0.6	2.50 ± 0.10	31.15 ± 1.26	51.9 ± 2.1
1:0.8	4.65 ± 0.11	58.16 ± 1.49	64.6 ± 1.6

To evaluate the in vitro release profile of Dex (Figure 2D), we used a micelle:Dex feed weight ratio of 1:0.8 ratio and the dialysis method. Micelles presented almost no release in the first 24 h in PBS at 37 °C, with a maximum release of 20% after 5 days. In contrast, the addition of GR enzyme at 50 mU induced a burst release, with ∼80% of the drug released in the first 24 h. In addition, although the size of the polymeric micelles did not significantly increase after 4 days in PBS, the addition of GR enzyme promoted the destabilization and degradation of the polymeric micelles (Table 2). Hence, these results highlight the sensitive behavior of the drug release from the polymeric micelles in the presence of GR enzyme.

Biological Assays. *Cytocompatibility of the Polymeric Micelles.* In vitro cell studies were performed to assess the viability of relevant cells that can be affected by this delivery device. Considering the synovial cavities the main site of therapeutic action, primary hACs from diseased knee arthroplasties (phenotype associated with arthritis disease), endothelial cells (main cells of the blood vessels), and macrophages (immune system) were used. All cells tested showed excellent cytocompatibility of the micelles below a concentration of 50 μg/mL (Figure 3). Considering the hACs and EA cell line, the cell viability, DNA quantification, and protein expression were not negatively affected for concentrations below 50 μg/mL. Above this concentration, there was a significant reduction in cell cytocompatibility in comparison with the control. For the THP-1 cell line, none of the concentrations reduce the cell viability, but there was a reduction in the DNA and protein quantification above 100 μg/mL. As the THP-1 cell line does not replicate, it was also observed that the amount of DNA and total protein expression in all tested conditions (including the control) decayed over time. Moreover, the cells morphology confirmed that they were not affected by the presence of the micelles even for

concentrations of 100 μg/mL (Figure 4). Thus, the maximum concentration of the polymeric micelles that does not harm the cells is 50 μg/mL.

Nevertheless, the analyses of the hemolytic properties of the polymeric micelles showed an absence of hemolysis at all the tested concentrations (Table 3), which demonstrated their in vitro hemocompatibility.

Dex Biological Effects in Monocultures and Coculture of hACs and THP-1. To compare the biological effects of the micelles encapsulating Dex with the free Dex, hACs and activated M1 macrophages in monoculture and coculture were used. The concentration of Dex was 100 μM, and in the coculture system, 50 mU of GR enzyme was added to the culture medium to mimic the synovial inflammation microenvironment.

The hACs viability and proliferation were significantly reduced with the addition of free Dex (Figure 5A). Interestingly, Dex encapsulation into the micelles was able to block the Dex negative effects over hACs, as there are no differences between the Ctr and Mic+Dex groups. Also, morphological analyses (Figure 6A) show that Mic+Dex did not influence the cell density nor the morphology of the hACs as observed in the Dex group. This effect was also observed in the THP-1 cell line (Figure 5B), where the presence of micelles promoted higher cell viability and proliferation in comparison with free Dex treatment.

The coculture of hACs with activated M1 macrophages significantly reduced the cell viability and proliferation in comparison to the hACs control (Figure 5A). While the treatment with Mic+Dex was able to reduce this harmful effect over the chondrocytes, the treatment with free Dex was not. Indeed, the Mic+Dex treatment significantly increases the cell viability in comparison with the coculture without treatment. These results were corroborated with the morphological analyses of the hACs (Figure 6B). After 14 days, the hACs presented altered morphology with cell shrinkage and a reduction of cell density. The treatment with the micelles encapsulating Dex was able to prevent these features more effectively than the free Dex. Additionally, the coculture system does not present negative effects over THP-1 cells, but the addition of the Mic+Dex and Dex significantly reduced the amount of DNA, especially after 1 day of treatment.

The coculture of hACs and activated M1 macrophages had a huge impact on the amount of TNF-α and IL-6 cytokines (Figure 5C, 5D, respectively) produced by those cells. Although hACs almost do not produce TNF-α, the yield of the activated M1 macrophages was around 1.3 ng/mL after 1 day, which was reduced to 0.1 ng/mL after 14 days. Despite all conditions (Ctr, Mic+Dex, and Dex in THP-1) presented a similar reduction of the TNF-α cytokine in the medium, in the

Table 2. Size Distribution (size, nm; and polydispersity index, PDI) of the Polymeric Micelles When Exposed to Different Environments: PBS and 50 mU of Glutathione Reductase (GR) enzyme at 37 °C

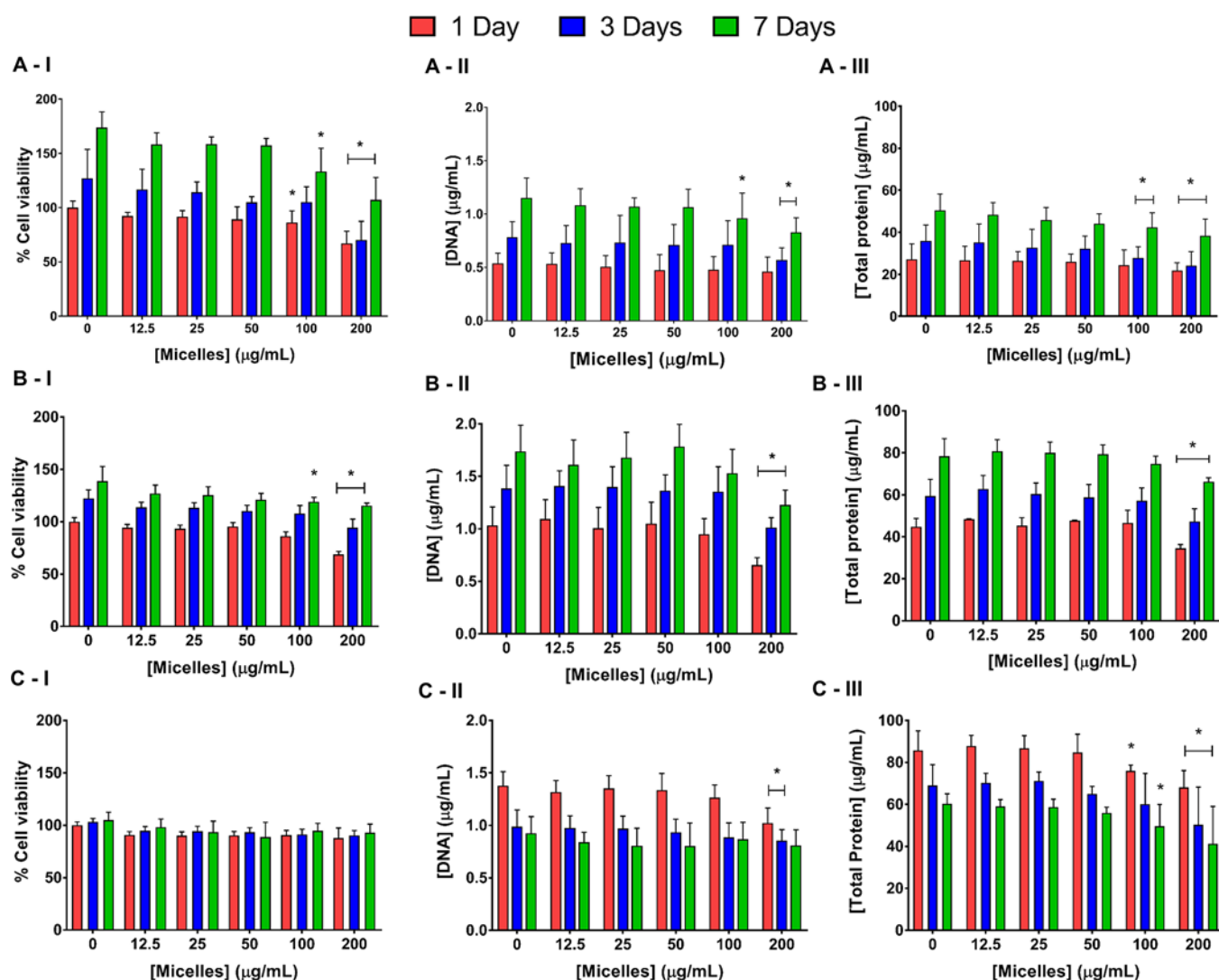|	PBS		50 mU GR[a]	
conditions	size (nm)	PDI	size (nm)	PDI
0 h	118.8 ± 0.18	0.105 ± 0.009	118.8 ± 0.18	0.105 ± 0.009
24 h	121.7 ± 3.45	0.121 ± 0.010	*	*
48 h	129.3 ± 1.56	0.155 ± 0.015	*	*
72 h	134.6 ± 2.15	0.177 ± 0.011	*	*
96 h	140.4 ± 1.26	0.195 ± 0.021	*	*

[a]* = No peak detected.

Figure 3. Biological performance: (I) cell viability, (II) cell proliferation, and (III) total protein synthesis, of the (A) hACs, (B) EA cell line, and (C) THP-1 cell line after 1, 3, and 7 days of culture with different concentrations of the polymeric micelles. Asterisk (*) indicates significant differences ($p < 0.01$) in comparison with the control (0 μg/mL).

coculture system, Mic+Dex were able to reduce it more than the free Dex, especially after 3 days. This result can be explained through the GR controlled release of the Dex from the micelles over time. Regarding the IL-6, the establishment of the coculture system increased the expression of this cytokine to a maximum of ∼1.2 μg/mL. Herein, both Mic+Dex and free Dex were capable to effectively reduce the amount of IL-6 cytokine in the medium to ∼0.1 μg/mL.

Considering that one of the biggest problems of GCs treatment is the negative effects over normal cells, the produced polymeric micelles were able to protect the chondrocytes from those effects. Moreover, the drug therapeutic effects were maintained after its encapsulation into the micelles. Therefore, the initial hypothesis was confirmed, as the developed polymeric micelles can prolong and extend the drug's half-life, increase its therapeutic efficacy, and decrease the side effects.

■ DISCUSSION

An efficient DDS should facilitate a stable circulation in plasma and release the drug in therapeutic concentrations at the diseased site. Hence, novel polymeric micelles were developed for controlled drug release in inflammatory conditions. The oxidation of the adjacent GSH in the micelles avoids the leakage of the drug into the plasma, as the disulfide cross-linking provides a barrier against blood dilution. After systemic administration, the accumulation in the inflammatory site (passive targeting) will trigger the controlled drug release by GR activity. Thus, this innovative technology was designed to (i) increase the therapeutic index of the drug through its encapsulation into the micelles; (ii) reduce the nefarious side effects of the drug due to the controlled release profiles, and consequently, reduce their unnecessary exposure to healthy tissues; and (iii) maximize the performance of the currently used therapies. Our results demonstrate that mPEG-GSH$_n$-PA micelles are an efficient DDS for the treatment of inflammatory arthritis.

In the ^{1}H NMR spectra the presence of the peaks of single compounds and the shifts in the carbons adjacent to the formed amide bond in the micelles spectrum confirmed the synthesis of the amphipathic polymer. This result was also corroborated by the shift of the NH$_2$ group from the mPEG and GSH and the COOH group of the PA and GSH to amide in the micelles in FTIR spectra. In the first reaction, the
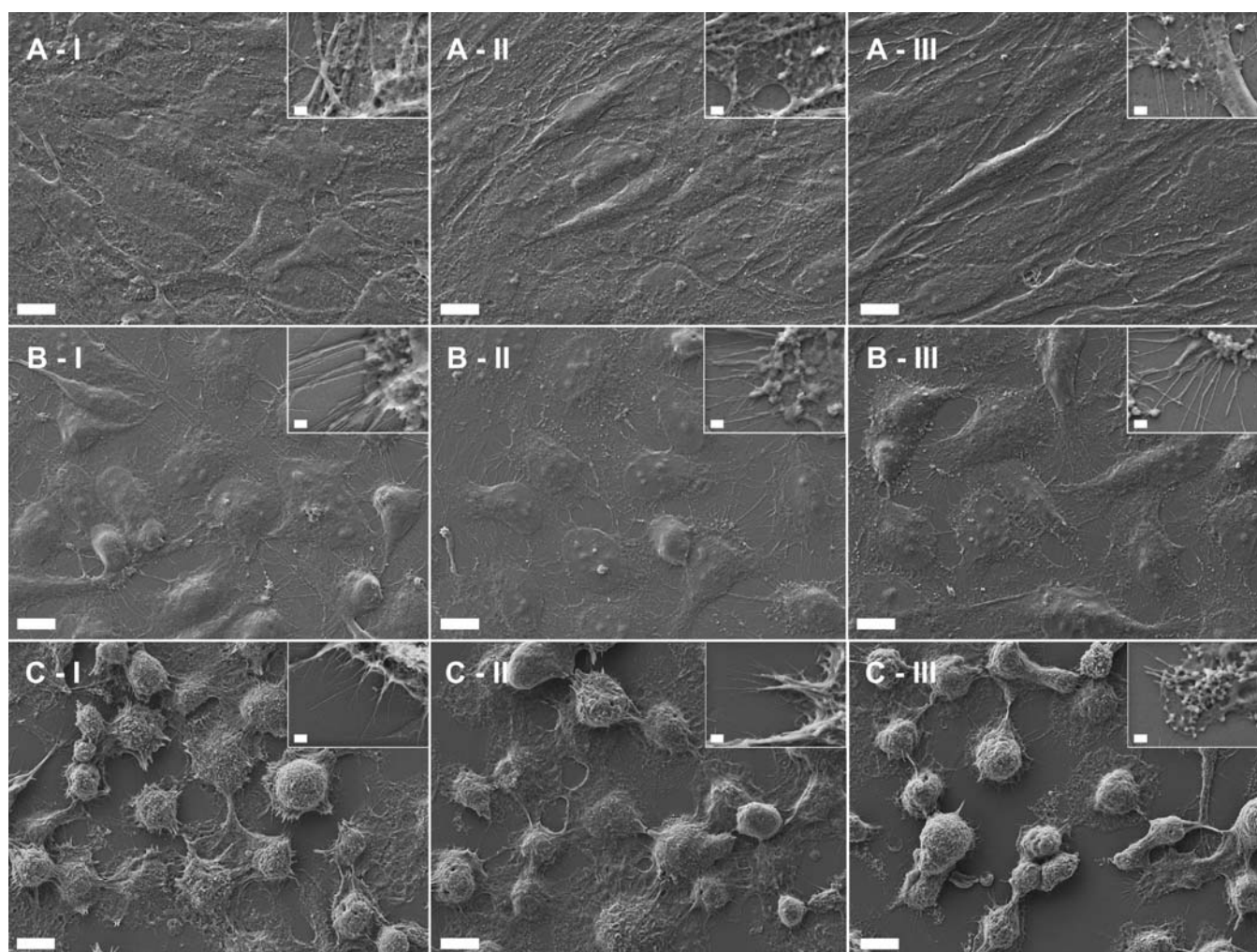
Figure 4. SEM microphotographs of the micelles cultured with (A) hACs, (B) EA cell line, and (C) THP-1 cell line in the absence (control, I) and presence of the micelles at different concentrations: (II) 50 and (III) 100 μg/mL. Scale bar 10 μm.

Table 3. Percentage of Hemolysis Provided by the Micelles in Contact with Blood Cells

samples	% hemolysis
control +	100
micelles at 12.5 μg/mL	0
micelles at 25 μg/mL	0
micelles at 50 μg/mL	0
micelles at 100 μg/mL	0
micelles at 200 μg/mL	0

mPEG-GSH grafted polymer was synthesized via the reaction of the NH_2 group of mPEG with the COOH group of GSH using EDC/NHS chemistry.[36] However, as free NH_2 groups of GSH can also react with the activated COOH group of GSH, the polymer can have more than one GSH linked to mPEG (mPEG-GSH$_n$), which will be further oxidized intermolecularly to retain the drug inside the resulting micelles. This reaction is nontoxic as the remaining products and byproducts (isourea) can be easily removed through dialysis with water,[37] which was performed after the first reaction was completed. In the second step, TBTU in the presence of the catalytic TEA promotes the reaction between the COOH group of PA with the NH_2 group of the mPEG-GSH$_n$ polymer to form an amide bond.[38] After the synthesis of the polymer mPEG-GSH$_n$-PA, polymeric micelles were successfully prepared through the nano-precipitation method.[39] Because it is an easy, quick, and one-step technique that can be easily scaled up, the nano-precipitation method is widely used to prepare a variety of NPs systems, including micelles.[40]

Stable polymeric micelles presented a size of 101.3 $\pm$ 3.4 nm, a PDI of 0.092 $\pm$ 0.011, and a zeta potential of $-20.2 \pm$ 3.42 mV. The size range around 100 nm enables the micelles to take advantage of the ELVIS mechanism and accumulate at inflamed joints.[41] Indeed, inflamed tissues present increased intraendothelial gaps due to the expression of histamine, bradykinin, leukotrienes, and serotonin that promotes the contraction of the inflammatory cells covering the capillaries. This effect has been widely explored not only for inflammatory conditions but also for cancer therapies (enhanced permeability and retention − EPR effect).[42] The PDI value lower than 0.2 confirmed their monodispersitivity in terms of size.[43] Considering the reduced absorption of the serum proteins to neutral and negative particles, the negative value of the zeta potential measurements further contributes to a prolonged circulation in the bloodstream.[44] Moreover, the value of the zeta potential of -20 mV ensures a stable particle suspension.[45] The size stability of the micelles was also confirmed during 6 months.
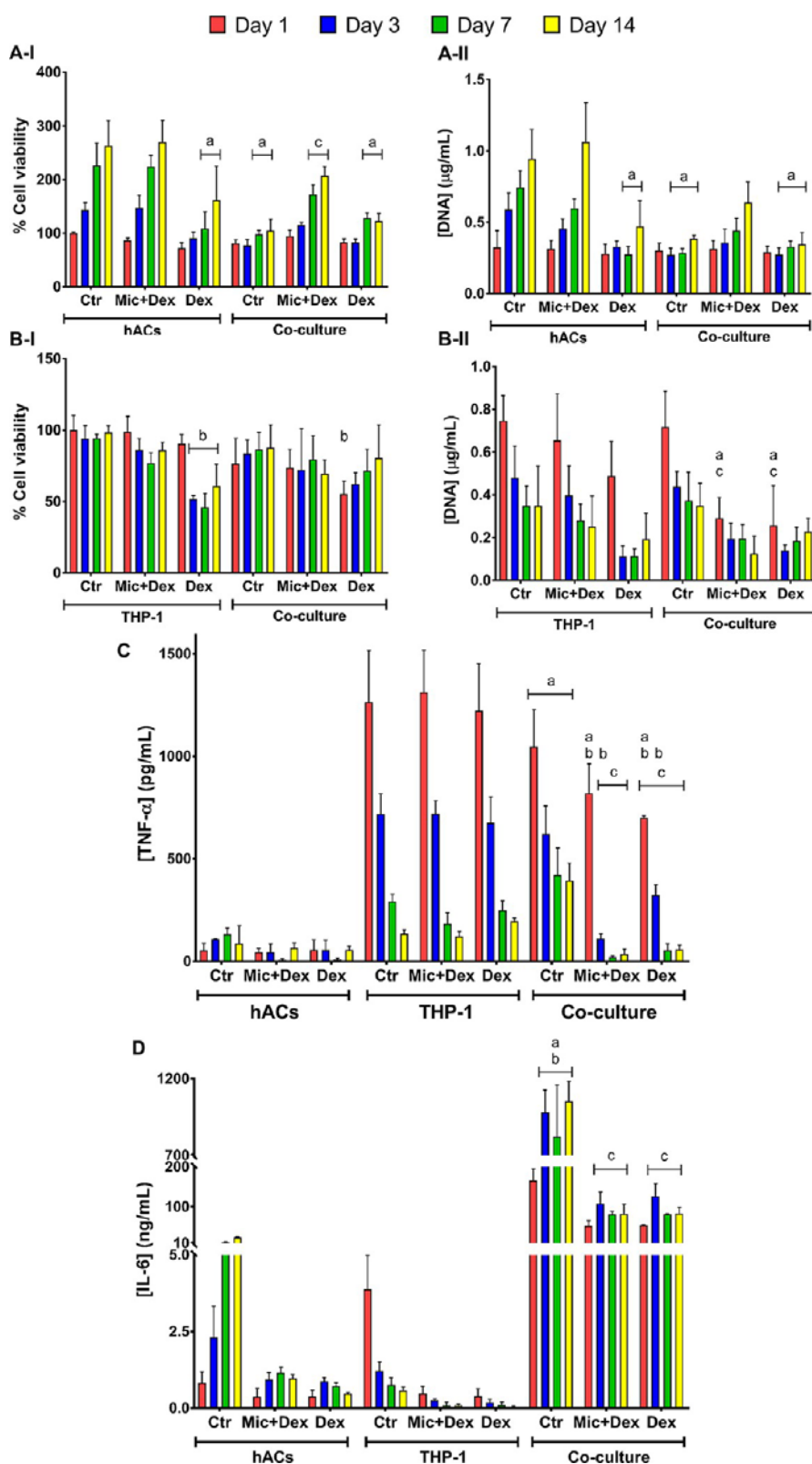
Figure 5. Biochemical performance: (I) cell viability and (II) cell proliferation of (A) hACs and (B) THP-1 cultured in monolayers and hACs cocultured with activated M1 macrophages after 1, 3, 7, and 14 days of treatment with different conditions: control (Ctr, no treatment), micelles encapsulating Dex (Mic+Dex) and Dex. The samples were also analyzed regarding (C) TNF-α concentration, and (D) IL-6 concentration. The alphabet "a" indicates significant difference in comparison with hACs Ctr, "b" indicates significant difference in comparison with to THP-1 Ctr, and "c" indicates significant difference in comparison with coculture Ctr, where $p < 0.01$.

Polymeric micelles exhibited a high Dex loading capacity that increased with the increment of the micelle:Dex feed

weight ratio. Indeed, the maximum entrapment efficiency (64%) occurred for the micelles:Dex feed weight ratio of 1:0.8
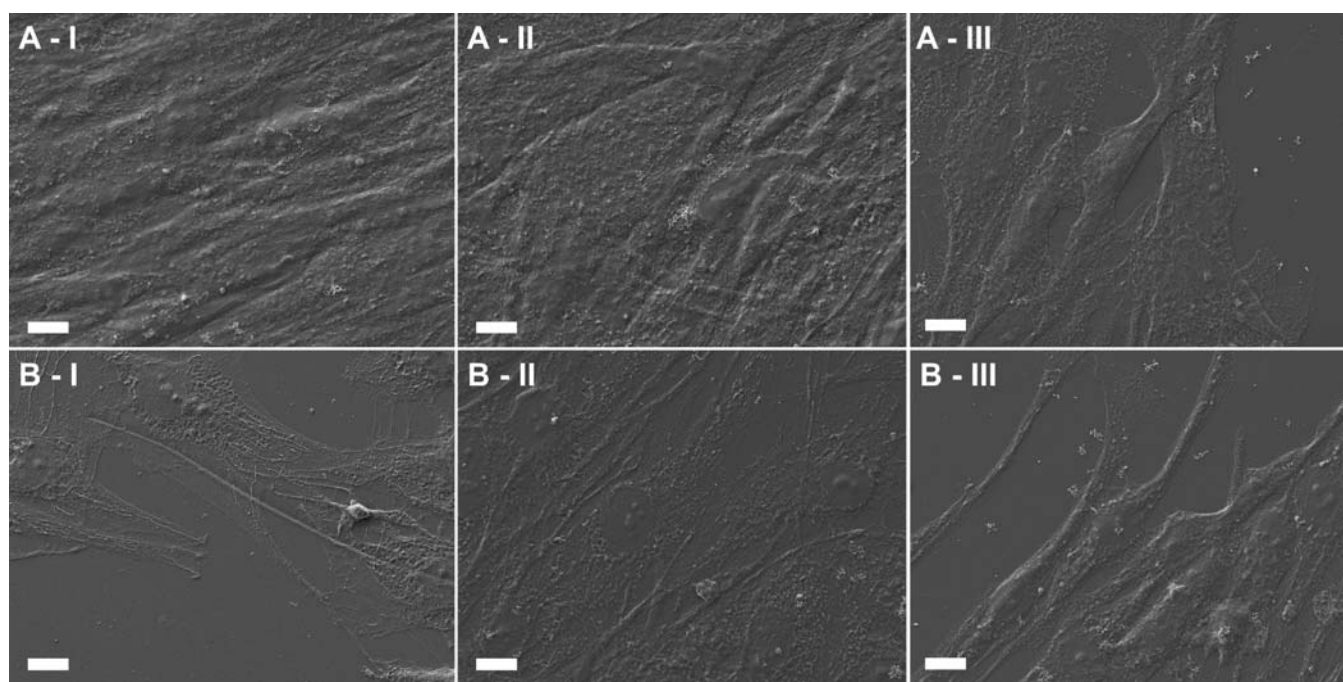
Figure 6. SEM microphotographs of (A) hACs cultured in monolayer and cocultured with (B) activated M1 macrophages after 14 days of treatment with different conditions: (I) no treatment, (II) micelles encapsulating Dex and (III) free Dex. Scale bars: 10 μm.

that comprises 4.65 ± 0.11 mg of Dex. Therefore, the amount of Dex present in the micelles is adequate to decrease the inflammatory process.[46] The kinetics of Dex release from the micelles is slow and low in PBS at 37 °C. While encapsulating the drug, the free thiol groups of GSH present into the amphiphilic polymer were oxidized by oxygen to form disulfide linkages, which prevent drug leakage. In the presence of the GR enzyme, there is a dissociation of the disulfide linkages and, consequently, a fast release of the drug. These results ensure a suitable amount of the drug into the polymeric micelles, as well as their stimuli-responsive properties under specific inflammatory conditions.

The in vitro cytotoxicity of the produced micelles was performed on endothelial cells, chondrocytes, and immune cells. EA cell line were used as a model of the cells lining the interior of the blood vessels, hACs isolated from diseased knee arthroplasties as a model of the target tissue, and THP-1 as a model of the immune system. Considering the rationale of the responsive micelles, all of these cell types represent a suitable model to assess any cytotoxic interaction after systemic administration. mPEG-GSH$_n$-PA micelles in a concentration until 50 μg/mL were cytocompatible in contact with hACs, EA, and THP-1 cells. As higher concentrations of the micelles negatively affected those cells, this was the maximum concentration of micelles used. Those results were comparable to other studies using amphiphilic polymers of PEG and other fatty acids or polymers.[47,48] The polymeric micelles did not influence cell morphology (SEM analysis). In addition, the hemocompatibility of the polymeric micelles was assessed using human blood, as it is a critical parameter before regulatory approval. Hence, considering the lack of hemolysis of the micelles in contact with red blood cells, according to the International Organization for Standardization (ISO/TR 7406) guidelines,[49] they are considered not hemolytic, and consequently, hemocompatible.

To confirm the ability of the micelles in counteracting inflammation and Dex side effects, we investigated their effect on chondrocytes and macrophages in both monoculture and coculture systems. In fact, chondrocytes viability and proliferation were compromised with the addition of the free Dex. Previous studies also reported a reduction in the chondrogenic cell line ATDC5 viability after Dex administration, due to the induction of autophagy.[50] Importantly, the micelles encapsulating the drug prevented those negative effects in the hACs. Regarding the THP-1 cell line, whereas free Dex impairs cell viability and proliferation, its incorporation into the micelles also reduced those negative effects. To model the inflamed joints, a transwell system was used to coculture hACs with activated M1 macrophages,[51] being GR enzyme added to further mimic the synovial inflammation in arthritic diseases. This system enabled assessing if the drug-loaded micelles could circumvent the deleterious impact of inflammation on human chondrocytes. To obtain an inflammatory scenario, we activated macrophages to the M1 phenotype. Indeed, the higher amount of TNF-α and IL-6 in activated macrophages and in the coculture systems confirmed their induction to the pro-inflammatory phenotype.[9] Moreover, the amount of IL-6 was much higher than TNF-α, which is also in agreement with the values from arthritic patients plasma and synovial fluid.[52] In the coculture system only the micelles encapsulating Dex were able to avoid the negative effects of the inflammation into the chondrocytes, especially after 14 days. Moreover, the Dex-loaded micelles were able to more effectively reduce the production of the IL-6 cytokine by macrophages. Hence, the initial hypothesis was confirmed as the micelles in the presence of GR activity ensure a controlled drug release. In a previous study, different nanomedicine formulations of Dex were compared in an adjuvant-induced arthritis rat model.[23] A slow drug release kinetics of the formulations, especially the micelles, demonstrated high therapeutic activity and joint protection. Thus, this strategy

is able to enhance the therapeutic index of the drug by increasing the therapeutic efficacy while reducing the nefarious side effects. Additionally, decreasing the drug release kinetics might reduce the dosage needed, and consequently, systemic side effects can be further avoided.

CONCLUSION

In conclusion, we developed enzymatic-sensitive polymeric micelles for controlled drug release on arthritic diseases. As our results clearly demonstrated a controlled drug release in the presence of GR enzyme, an increase of its therapeutic efficacy in specific tissues is ensured, and consequently, a reduction of off-target effects can be expected. Hence, the developed device allows overcoming some drawbacks of current treatments, such as the limited solubility and efficacy of the drug, its inadequate pharmacokinetics, and its severe side effects. Therefore, the polymeric micelles are a valid approach not only for arthritic diseases but also for other inflammatory conditions.

AUTHOR INFORMATION

Corresponding Author

Nuno M. Neves − 3B's Research Group, I3Bs — Research Institute on Biomaterials, Biodegradables and Biomimetics, University of Minho, Headquarters of the European Institute of Excellence on Tissue Engineering and Regenerative Medicine, Barco 4805-017, Guimarães, Portugal; ICVS/3B's—PT Government Associate Laboratory, Braga, Guimarães, Portugal; orcid.org/0000-0003-3041-0687; Email: nuno@i3bs.uminho.pt

Authors

Ana Cláudia Lima − 3B's Research Group, I3Bs — Research Institute on Biomaterials, Biodegradables and Biomimetics, University of Minho, Headquarters of the European Institute of Excellence on Tissue Engineering and Regenerative Medicine, Barco 4805-017, Guimarães, Portugal; ICVS/3B's—PT Government Associate Laboratory, Braga, Guimarães, Portugal; orcid.org/0000-0002-9102-6235

Rui L. Reis − 3B's Research Group, I3Bs — Research Institute on Biomaterials, Biodegradables and Biomimetics, University of Minho, Headquarters of the European Institute of Excellence on Tissue Engineering and Regenerative Medicine, Barco 4805-017, Guimarães, Portugal; ICVS/3B's—PT Government Associate Laboratory, Braga, Guimarães, Portugal

Helena Ferreira − 3B's Research Group, I3Bs — Research Institute on Biomaterials, Biodegradables and Biomimetics, University of Minho, Headquarters of the European Institute of Excellence on Tissue Engineering and Regenerative Medicine, Barco 4805-017, Guimarães, Portugal; ICVS/3B's—PT Government Associate Laboratory, Braga, Guimarães, Portugal

Complete contact information is available at:
https://pubs.acs.org/10.1021/acsbiomaterials.1c00412

Author Contributions

The manuscript was written through contributions of all authors. All authors have given approval to the final version of the manuscript.

Notes

ACKNOWLEDGMENTS

REFERENCES

(1) Lektrakul, N.; Chung, C. B.; Resnick, D. Arthritis. In *Imaging of the Shoulder*; Springer: Berlin, 2006; pp 223−233.

(2) Roy, K.; Kanwar, R. K.; Kanwar, J. R. Molecular targets in arthritis and recent trends in nanotherapy. *Int. J. Nanomed.* **2015**, *10*, 5407−5420.

(3) Rubin, R. EULAR: Countries unite to fight rheumatic diseases. *Lancet* **2017**, *389* (10086), 2276.

(4) Ledingham, J.; Snowden, N.; Ide, Z. Diagnosis and early management of inflammatory arthritis. *Br. Med. J.* **2017**, *358*, j3248.

(5) Geenen, R.; Overman, C. L.; Christensen, R.; Asenlof, P.; Capela, S.; Huisinga, K. L.; Husebo, M. E. P.; Koke, A. J. A.; Paskins, Z.; Pitsillidou, I. A.; et al. EULAR recommendations for the health professional's approach to pain management in inflammatory arthritis and osteoarthritis. *Ann. Rheum. Dis.* **2018**, *77* (6), 797−807.

(6) Vandewalle, J.; Luypaert, A.; De Bosscher, K.; Libert, C. Therapeutic Mechanisms of Glucocorticoids. *Trends Endocrinol. Metab.* **2018**, *29* (1), 42−54.

(7) Cabral, H.; Miyata, K.; Osada, K.; Kataoka, K. Block Copolymer Micelles in Nanomedicine Applications. *Chem. Rev.* **2018**, *118* (14), 6844−6892.

(8) Petros, R. A.; DeSimone, J. M. Strategies in the design of nanoparticles for therapeutic applications. *Nat. Rev. Drug Discovery* **2010**, *9* (8), 615−627.

(9) Lima, A. C.; Cunha, C.; Carvalho, A.; Ferreira, H.; Neves, N. M. Interleukin-6 Neutralization by Antibodies Immobilized at the Surface of Polymeric Nanoparticles as a Therapeutic Strategy for Arthritic Diseases. *ACS Appl. Mater. Interfaces* **2018**, *10* (16), 13839−13850.

(10) Lima, A. C.; Amorim, D.; Laranjeira, I.; Almeida, A.; Reis, R. L.; Ferreira, H.; Pinto-Ribeiro, F.; Neves, N. M. Modulating inflammation through the neutralization of Interleukin-6 and tumor necrosis factor-α by biofunctionalized nanoparticles. *J. Controlled Release* **2021**, *331*, 491−502.

(11) Lima, A. C.; Campos, C. F.; Cunha, C.; Carvalho, A.; Reis, R. L.; Ferreira, H.; Neves, N. M. Biofunctionalized Liposomes to Monitor Rheumatoid Arthritis Regression Stimulated by Interleukin-23 Neutralization. *Adv. Healthcare Mater.* **2021**, *10* (2), e2001570.

(12) Jhaveri, A. M.; Torchilin, V. P. Multifunctional polymeric micelles for delivery of drugs and siRNA. *Front. Pharmacol.* **2014**, *5*, 1−26.

(13) Nicolas, J.; Mura, S.; Brambilla, D.; Mackiewicz, N.; Couvreur, P. Design, functionalization strategies and biomedical applications of targeted biodegradable/biocompatible polymer-based nanocarriers for drug delivery. *Chem. Soc. Rev.* **2013**, *42* (3), 1147−235.

(14) Kataoka, K.; Harada, A.; Nagasaki, Y. Block copolymer micelles for drug delivery: design, characterization and biological significance. *Adv. Drug Delivery Rev.* **2001**, *47* (1), 113−131.

(15) Lima, A. C.; Ferreira, H.; Reis, R. L.; Neves, N. M. Biodegradable polymers: an update on drug delivery in bone and cartilage diseases. *Expert Opin. Drug Delivery* **2019**, *16* (8), 795−813.

(16) Kamaly, N.; Yameen, B.; Wu, J.; Farokhzad, O. C. Degradable Controlled-Release Polymers and Polymeric Nanoparticles: Mechanisms of Controlling Drug Release. *Chem. Rev.* **2016**, *116* (4), 2602−2663.

(17) Pu, H. L.; Chiang, W. L.; Maiti, B.; Liao, Z. X.; Ho, Y. C.; Shim, M. S.; Chuang, E. Y.; Xia, Y. N.; Sung, H. W. Nanoparticles with Dual Responses to Oxidative Stress and Reduced pH for Drug Release and Anti-inflammatory Applications. *ACS Nano* **2014**, *8* (2), 1213−1221.

(18) Lu, S. C. Regulation of glutathione synthesis. *Mol. Aspects Med.* **2009**, *30* (1−2), 42−59.

(19) Nash, K. M.; Ahmed, S. Nanomedicine in the ROS-mediated pathophysiology: Applications and clinical advances. *Nanomedicine* **2015**, *11* (8), 2033−40.

(20) Ostalowska, A.; Birkner, E.; Wiecha, M.; Kasperczyk, S.; Kasperczyk, A.; Kapolka, D.; Zon-Giebel, A. Lipid peroxidation and antioxidant enzymes in synovial fluid of patients with primary and secondary osteoarthritis of the knee joint. *Osteoarthr Cartilage* **2006**, *14* (2), 139−145.

(21) Sredzinska, K.; Galicka, A.; Porowska, H.; Sredzinski, L.; Porowski, T.; Popko, J. Glutathione reductase activity correlates with concentration of extracellular matrix degradation products in synovial fluid from patients with joint diseases. *Acta Biochim Pol* **2009**, *56* (4), 635−40.

(22) Wang, Q.; Jiang, J. Y.; Chen, W. F.; Jiang, H.; Zhang, Z. R.; Sun, X. Targeted delivery of low-dose dexamethasone using PCL-PEG micelles for effective treatment of rheumatoid arthritis. *J. Controlled Release* **2016**, *230*, 64−72.

(23) Quan, L.; Zhang, Y.; Crielaard, B. J.; Dusad, A.; Lele, S. M.; Rijcken, C. J. F.; Metselaar, J. M.; Kostkova, H.; Etrych, T.; Ulbrich, K.; Kiessling, F.; Mikuls, T. R.; Hennink, W. E.; Storm, G.; Lammers, T.; Wang, D. Nanomedicines for inflammatory arthritis: head-to-head comparison of glucocorticoid-containing polymers, micelles, and liposomes. *ACS Nano* **2014**, *8* (1), 458−466.

(24) Kalyane, D.; Raval, N.; Maheshwari, R.; Tambe, V.; Kalia, K.; Tekade, R. K. Employment of enhanced permeability and retention effect (EPR): Nanoparticle-based precision tools for targeting of therapeutic and diagnostic agent in cancer. *Mater. Sci. Eng., C* **2019**, *98*, 1252−1276.

(25) Suk, J. S.; Xu, Q. G.; Kim, N.; Hanes, J.; Ensign, L. M. PEGylation as a strategy for improving nanoparticle-based drug and gene delivery. *Adv. Drug Delivery Rev.* **2016**, *99*, 28−51.

(26) Liu, X. M.; Quan, L. D.; Tian, J.; Laquer, F. C.; Ciborowski, P.; Wang, D. Syntheses of click PEG-dexamethasone conjugates for the treatment of rheumatoid arthritis. *Biomacromolecules* **2010**, *11* (10), 2621−8.

(27) Ma, Y. F.; Wang, L. J.; Zhou, Y. L.; Zhang, X. X. A facilely synthesized glutathione-functionalized silver nanoparticle-grafted covalent organic framework for rapid and highly efficient enrichment of N-linked glycopeptides. *Nanoscale* **2019**, *11* (12), 5526−5534.

(28) Kim, H. C.; Kim, E.; Ha, T. L.; Lee, S. G.; Lee, S. J.; Jeong, S. W. Highly stable and reduction responsive micelles from a novel polymeric surfactant with a repeating disulfide-based gemini structure for efficient drug delivery. *Polymer* **2017**, *133*, 102−109.

(29) Quinn, J. F.; Whittaker, M. R.; Davis, T. P. Glutathione responsive polymers and their application in drug delivery systems. *Polym. Chem.* **2017**, *8* (1), 97−126.

(30) Zhang, H. Y.; Sun, C. Y.; Adu-Frimpong, M.; Yu, J. N.; Xu, X. M. Glutathione-sensitive PEGylated curcumin prodrug nanomicelles:

Preparation, characterization, cellular uptake and bioavailability evaluation. *Int. J. Pharmaceut.* **2019**, *555*, 270−279.

(31) Thotakura, N.; Dadarwal, M.; Kumar, R.; Singh, B.; Sharma, G.; Kumar, P.; Katare, O. P.; Raza, K. Chitosan-palmitic acid based polymeric micelles as promising carrier for circumventing pharmacokinetic and drug delivery concerns of tamoxifen. *Int. J. Biol. Macromol.* **2017**, *102*, 1220−1225.

(32) Huang, Y. H.; Jazani, A. M.; Howell, E. P.; Reynolds, L. A.; Oh, J. K.; Moffitt, M. G. Microfluidic Shear Processing Control of Biological Reduction Stimuli-Responsive Polymer Nanoparticles for Drug Delivery. *ACS Biomater. Sci. Eng.* **2020**, *6* (9), 5069−5083.

(33) Rahman, I.; Kode, A.; Biswas, S. K. Assay for quantitative determination of glutathione and glutathione disulfide levels using enzymatic recycling method. *Nat. Protoc.* **2006**, *1* (6), 3159−3165.

(34) Sversut, R. A.; Vieira, J. C.; Rosa, A. M.; Singh, A. K.; do Amaral, M. S.; Kassab, N. M. Improved UV Spectrophotometric Method for Precise, Efficient and Selective Determination of Dexamethasone in Pharmaceutical Dosage Forms. *Orbital: Electron. J. Chem.* **2015**, *7* (1), 5−9.

(35) Alves da Silva, M. L.; Costa-Pinto, A. R.; Martins, A.; Correlo, V. M.; Sol, P.; Bhattacharya, M.; Faria, S.; Reis, R. L.; Neves, N. M. Conditioned medium as a strategy for human stem cells chondrogenic differentiation. *J. Tissue Eng. Regener. Med.* **2015**, *9* (6), 714−723.

(36) Pieper, J. S.; Hafmans, T.; Veerkamp, J. H.; van Kuppevelt, T. H. Development of tailor-made collagen-glycosaminoglycan matrices: EDC/NHS crosslinking, and ultrastructural aspects. *Biomaterials* **2000**, *21* (6), 581−593.

(37) Ahmad, Z.; Shepherd, J. H.; Shepherd, D. V.; Ghose, S.; Kew, S. J.; Cameron, R. E.; Best, S. M.; Brooks, R. A.; Wardale, J.; Rushton, N. Effect of 1-ethyl-3-(3-dimethylaminopropyl) carbodiimide and N-hydroxysuccinimide concentrations on the mechanical and biological characteristics of cross-linked collagen fibres for tendon repair. *Regenerative biomaterials* **2015**, *2* (2), 77−85.

(38) Montalbetti, C. A. G. N.; Falque, V. Amide bond formation and peptide coupling. *Tetrahedron* **2005**, *61* (46), 10827−10852.

(39) Fessi, H.; Puisieux, F.; Devissaguet, J. P.; Ammoury, N.; Benita, S. Nanocapsule Formation by Interfacial Polymer Deposition Following Solvent Displacement. *Int. J. Pharm.* **1989**, *55* (1), R1−R4.

(40) Rivas, C. J. M.; Tarhini, M.; Badri, W.; Miladi, K.; Greige-Gerges, H.; Nazari, Q. A.; Rodriguez, S. A. G.; Roman, R. A.; Fessi, H.; Elaissari, A. Nanoprecipitation process: From encapsulation to drug delivery. *Int. J. Pharmaceut.* **2017**, *532* (1), 66−81.

(41) Nehoff, H.; Parayath, N. N.; Domanovitch, L.; Taurin, S.; Greish, K. Nanomedicine for drug targeting: strategies beyond the enhanced permeability and retention effect. *Int. J. Nanomed.* **2014**, *9*, 2539−2555.

(42) Golombek, S. K.; May, J. N.; Theek, B.; Appold, L.; Drude, N.; Kiessling, F.; Lammers, T. Tumor targeting via EPR: Strategies to enhance patient responses. *Adv. Drug Delivery Rev.* **2018**, *130*, 17−38.

(43) Panchal, J.; Kotarek, J.; Marszal, E.; Topp, E. M. Analyzing subvisible particles in protein drug products: a comparison of dynamic light scattering (DLS) and resonant mass measurement (RMM). *AAPS J.* **2014**, *16* (3), 440−51.

(44) Blanco, E.; Shen, H.; Ferrari, M. Principles of nanoparticle design for overcoming biological barriers to drug delivery. *Nat. Biotechnol.* **2015**, *33* (9), 941−951.

(45) Bhattacharjee, S. DLS and zeta potential - What they are and what they are not? *J. Controlled Release* **2016**, *235*, 337−51.

(46) Hochhaus, G.; Barth, J.; Al-Fayoumi, S.; Suarez, S.; Derendorf, H.; Hochhaus, R.; Mollmann, H. Pharmacokinetics and pharmacodynamics of dexamethasone sodium-m-sulfobenzoate (DS) after intravenous and intramuscular administration: A comparison with dexamethasone phosphate (DP). *J. Clin. Pharmacol.* **2001**, *41* (4), 425−434.

(47) Li, Y.; Xiao, K.; Luo, J.; Xiao, W.; Lee, J. S.; Gonik, A. M.; Kato, J.; Dong, T. A.; Lam, K. S. Well-defined, reversible disulfide cross-linked micelles for on-demand paclitaxel delivery. *Biomaterials* **2011**, *32* (27), 6633−45.

(48) Gardey, E.; Sobotta, F. H.; Hoeppener, S.; Bruns, T.; Stallmach, A.; Brendel, J. C. Influence of Core Cross-Linking and Shell Composition of Polymeric Micelles on Immune Response and Their Interaction with Human Monocytes. *Biomacromolecules* **2020**, *21* (4), 1393−1406.

(49) Henkelman, S.; Rakhorst, G.; Blanton, J.; van Oeveren, W. Standardization of incubation conditions for hemolysis testing of biomaterials. *Mater. Sci. Eng., C* **2009**, *29* (5), 1650−1654.

(50) Zhao, Y.; Zuo, Y.; Huo, H.; Xiao, Y.; Yang, X.; Xin, D. Dexamethasone reduces ATDC5 chondrocyte cell viability by inducing autophagy. *Mol. Med. Rep.* **2014**, *9* (3), 923−7.

(51) Bauer, C.; Niculescu-Morzsa, E.; Jeyakumar, V.; Kern, D.; Späth, S. S.; Nehrer, S. Chondroprotective effect of high-molecular-weight hyaluronic acid on osteoarthritic chondrocytes in a co-cultivation inflammation model with M1 macrophages. *J. Inflammation (London, U. K.)* **2016**, *13* (31), 1−9.

(52) Mabey, T.; Honsawek, S.; Tanavalee, A.; Yuktanandana, P.; Wilairatana, V.; Poovorawan, Y. Plasma and synovial fluid inflammatory cytokine profiles in primary knee osteoarthritis. *Biomarkers* **2016**, *21* (7), 639−44.